Airborne studies of correlation between the radiances of surface elements in some intervals of the 0.4–1.2 μm region

M.I. Allenov, A.I. Gusev, N.P. Ivanova, and V.V. Sulimov

Science and Production Association "Taifun,"
Obninsk, Kaluga Region

In this paper we present the results of our studies of correlation between the radiance fluctuations recorded along a 6-km long path in the spectral intervals with λ_{max} at 445, 540, 650, 800, and 1050 nm. The underflight paths crossed fields of cultivated plants, bare fallow, water surface, forest, etc. Stable features of the paths' radiance have been found that can occur under different meteorological conditions.

The correlation between fluctuations of the spectral density of the underlying surface elements radiance (forest, grass, soil, fields of cultivated plants, and others) under the variety of meteorological conditions was considered in Refs. 1 to 3. It turned out that the coefficients of correlation between the data of reference (primary) measurements and the measurements conducted under similar conditions (meteorological conditions, Sun elevation, time of day) but shifted in time by several days decreased significantly. Thus it was shown that to identify the state of surface elements, reference cases should be periodically introduced to provide a standard with which the subsequent measurements can be compared.

This paper presents the results of our study of the correlation calculated using airborne measurement data obtained for longer time.

To study the radiance characteristics of the surface elements, we have selected two flight routes (Table 1).

Table 1. Description of the flight routes

Route 1. South-east direction	Route 2. North-east direction
Forest	Forest
Bay	Bay
Forest	Forest
Field (winter wheat)	Field (winter wheat)
Dirt road	Forest
Field (fodder grass)	Field (oats)
Forest belt	Forest belt
Field (bare fallow)	Field (winter wheat)
Forest belt	Reservoir
Field (winter wheat)	–
Forest	–
Reservoir	–

The measurements were conducted with spectroradiometers in the intervals given in Table 2.

Table 2

Channel	λ_{max}, nm	$\Delta\lambda_{0.5}$, nm
1	445	34
2	540	43
3	650	42
4	800	60
5	1050	10

The length of a single path was 6 km. The spatial resolution on the underlying surface was, at the flight altitude of 100 m, on the average about 1.2 m. However, the presented results were digitized in 10 m.

Consider some peculiarities in the distribution of the spectral density of the radiance of different surface elements.

1. Water surface is characterized by relatively low spatial variations of spectral radiance in all channels of the spectrometer at the Sun elevation angles of 42 and 53° and under cloudy conditions. As the Sun elevation angle increases up to 59 and 65°, the level of radiance of the water surface in the visible spectral region increases sharply and the spatial inhomogeneity of the reflected radiation increases too. This is explained by the appearance of flashes from the water surface within a device's field of view at the high Sun.

2. Forested areas differ from other objects primarily by the high spatial inhomogeneity of the field of reflected radiation in the green and near infrared spectral regions. The scale of spatial variations is somewhat lower under conditions of illumination by scattered radiation under cloudy conditions as compared with that under clear skies.

3. Winter wheat is characterized by a significantly smaller scale of spatial variations of the reflected radiation as compared with the forest under conditions of both cloudy and clear skies.

4. Since the reflecting properties of the water surface vary widely in the visible spectral region, one can observe strong variations of the contrast (including the change of sign) between the water and plant canopy as the Sun elevation angle and meteorological conditions change. No marked changes in contrast between forest and winter wheat are observed under similar conditions.

5. In the case of broken clouds, variations of the spatial distribution of the illuminating radiation are noticeable, what causes significant changes in the spatial distribution of the reflected radiation along a flight route.

The characteristics of the surface elements of the second route are close to those of the first one, therefore they are not presented here.

As a reference, we took the shores of the bay and Kakhovskoe Reservoir itself.

The mathematical processing of information included the following steps. One of the flights along the route, usually on a day with fine weather, was taken as a reference one. Then the coefficients of correlation between the data of the reference flight and the rest flights were calculated for each spectral channel.

The calculations was made by the equation[3]:

$$r_{k,k_0,m} =$$

$$= \frac{\sum\limits_{i=1}^{N} B_i^{k,m}\, B_i^{k_0,m} - N\overline{B^{k,m}}\,\overline{B^{k_0,m}}}{\left\{\left[\sum\limits_{i=1}^{N}(B_i^{k,m})^2 - N(\overline{B^{k,m}})^2\right]\left[\sum\limits_{i=1}^{N}(B_i^{k_0,m})^2 - N(\overline{B^{k_0,m}})^2\right]\right\}^{\frac{1}{2}}},$$

where m is the number of the spectral interval (channel); k is the number of the flight over the route; k_0 is the number of the reference flight; $B_i^{k,m}$ and $B_i^{k_0,m}$ are the values of the spectral radiance at the ith point of a sample in the mth spectral interval in the kth and reference flights, respectively; $\overline{B^{k,m}}$ is the route mean value of the radiance in the mth spectral interval in the kth flight; $\overline{B^{k_0,m}}$ is the route mean value of radiance in the mth spectral interval in the reference flight; N is the number of readouts of radiance in samples.

To evaluate objectively the illumination conditions along the path for each flight from the spectroradiometric data, we calculated the coefficient of variation of the radiative flux V_k along the working segment of the route:

$$V_k = \frac{\left\{\dfrac{1}{N-1}\left[\sum\limits_{i=1}^{N}(E_i^k)^2 - N(\overline{E}^k)^2\right]\right\}^{1/2}}{\overline{E}^k},$$

where E_i^k is the value of the irradiance at the ith point of the sample in the kth flight; $\overline{E}_i^k$ is the mean value of the irradiance along the working section of the route in the kth flight.

As a reference, we have selected three flights for each of the routes on June 20, and July 18 and 26. These flights were performed under nearly cloudless conditions with no cloud shadows on the path. The results of processing of the airborne measurement data for the period from 10:00 to 13:00 (Moscow time) are shown in the figure.

As can be seen from the figure, for the first and second spectral intervals at the time shift with respect to the reference cases, the correlation weakens markedly in ten days. The weakening is also observed in the other spectral intervals. Correlation is most stable for the third channel (red spectral region). Similar tendency in the behavior of the correlation coefficients was noticed in Ref. 3 as well.

The results obtained as a function of the Sun elevation angle h_3 for every route and for every spectral interval show that strong correlation of the spatial distribution of the reflected radiation with the reference distribution occurs at the Sun elevation angles from 30 to 60°. The correlation coefficient exceeds, as a rule, 0.80–0.85. In some cases, at the highest and lowest positions of the Sun, the decrease in the value of $r_{k,k_0,m}$ was observed. However, this decrease was not stable.

Cloudiness has a strong effect on the distribution of the reflected radiation if it causes a significant deviation of illumination conditions from the homogeneous ones, in particular, in the presence of shadows along the path. If the path is uniformly illuminated, even under overcast conditions, when the surface is illuminated only by scattered radiation, close statistical correlation is observed between the spatial distribution of the reflected radiation and the reference distribution obtained under nearly cloudless conditions, when the path was illuminated by direct solar radiation.
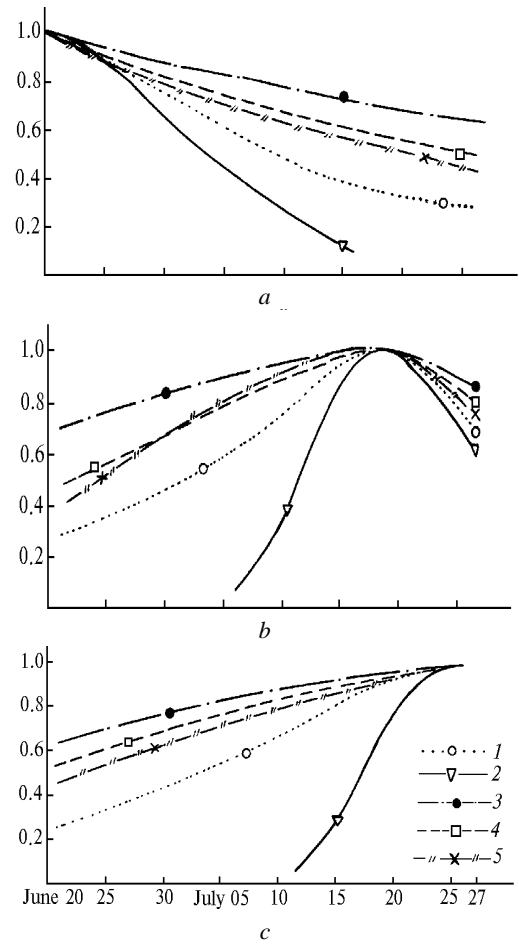
Fig. 1. Time dependence of the correlation coefficients for the reference routes on June 20 (*a*), July 18 (*b*), and July 26 (*c*): 436–460 (*1*), 522–565 (*2*), 634–680 (*3*), 762–822 (*4*), and 1045–1055 nm (*5*).

Passing to consideration of $r_{k,k_0,m}$ variations in time, let us note that the states of the objects changed significantly during the observation period: winter wheat on the first and fourth fields was harvested, and in the second half of the observation cycle the fields were stubble; fodder grass on the field 2 was mowed down and removed, and the field was ploughed up; the fallow field 3 was covered by weed by the end of the observation cycle. No marked changes in the state of the forest on the bay shore were observed.

Thus, significant changes were observed in the correlation coefficient between the spatial distributions of the reflected radiation obtained at different states of the objects (the observations were conducted in the black-earth zone, on the flat surface, along the route including a water surface, forest, and agricultural fields during the period including the ripening of grain crops, harvesting grain crops and ploughing). The maximum changes were observed in the green and blue spectral regions, whereas the minimum changes were observed in the red and near infrared regions.

**Table 3. Average correlation matrices
for flights along the route 1**

Date, time	Spectral region, nm				
	436–460	522–565	634–680	762–822	1045–1055
June 20,	1.00	0.84	0.85	0.07	0.26

10:50 a.m.		1.00	0.83	0.41	0.54
			1.00	0.24	0.43
				1.00	0.94
					1.00
July 18, 10:29 a.m.	1.00	0.89	0.90	0.04	0.34
		1.00	0.95	0.25	0.51
			1.00	0.01	0.46
				1.00	0.90
					1.00
July 26, 11:04 a.m.	1.00	0.82	0.93	0.29	0.47
		1.00	0.89	0.43	0.57
			1.00	0.37	0.55
				1.00	0.94
					1.00

In conclusion let us consider the correlation between the realizations of the spatial distribution of the reflected radiation in different spectral intervals within a single flight. This correlation can be described by a correlation matrix comprising the correlation coefficients between all pairs of spectral channels. Table 3 gives the calculated average correlation matrices for three flights along the route 1 and three flights along the route 2 at different states of the objects under conditions of uniform illumination.

As seen from the Table 3, the statistical correlation exists in these three periods with the high correlation coefficient ($r \geq 0.85$) for all combinations of the three channels in the visible spectral region: blue–green, blue–red, and green–red. High correlation coefficients ($r \geq 0.91$) were also obtained for two channels in the near infrared: 762–822 and 1045–1055 nm. At the same time, the correlation between the channels in the visible and the channels in the infrared is relatively weak; the coefficients of correlation between these channels for all the flights did not exceed 0.65.

References

1. M.I. Allenov, *Structure of Optical Radiation of Natural Objects* (Gidrometeoizdat, Moscow, 1988), 164 pp.
2. M.I. Allenov, S.N. Voyakin, A.D. Dobrozrakov, Yu.M. Kondrat'ev, and S.G. Yakovlev, Trudy IEM, Issue 20 (140), 34–45 (1989).
3. M.I. Allenov, A.I. Gusev, N.P. Ivanova, and V.V. Sulimov, Atmos. Oceanic. Opt. **12**, No. 2, 136–139 (1999).